Supplemental material

Lee et al., https://doi.org/10.1083/jcb.201711104

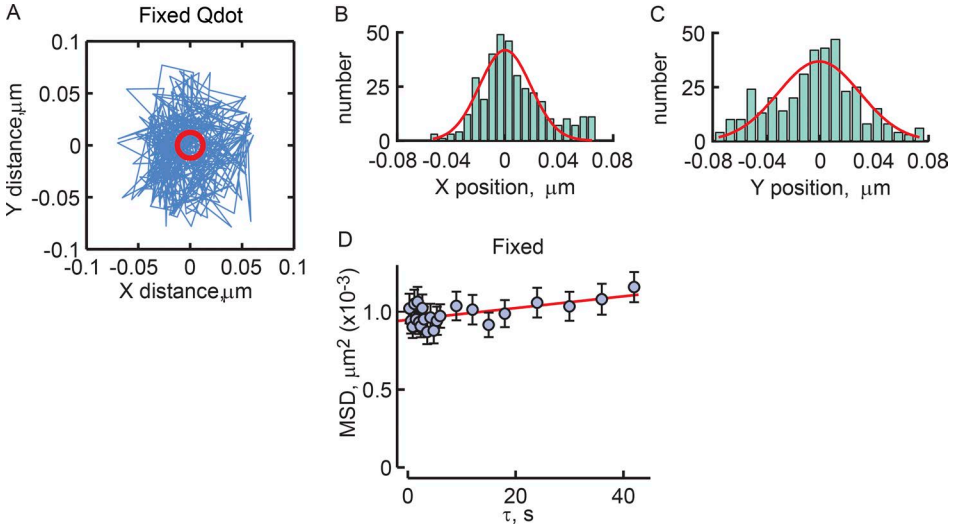

Figure S1. **Positional precision of the tracking system. (A)** x and y movements of a Qdot coupled to a GPCR after fixing with glutaraldehyde. **(B and C)** Positional histograms in the x and y dimensions from the results shown in A. Red lines are Gaussian fittings of the histograms. **(D)** MSD(τ) analysis of the Qdot-labeled Rhoi3S on a fixed cell. This plot represents the noise in the measurements that is subtracted from the MSD(τ) results. Markers represent mean ± SEM. *n* = 13; three independent experiments.

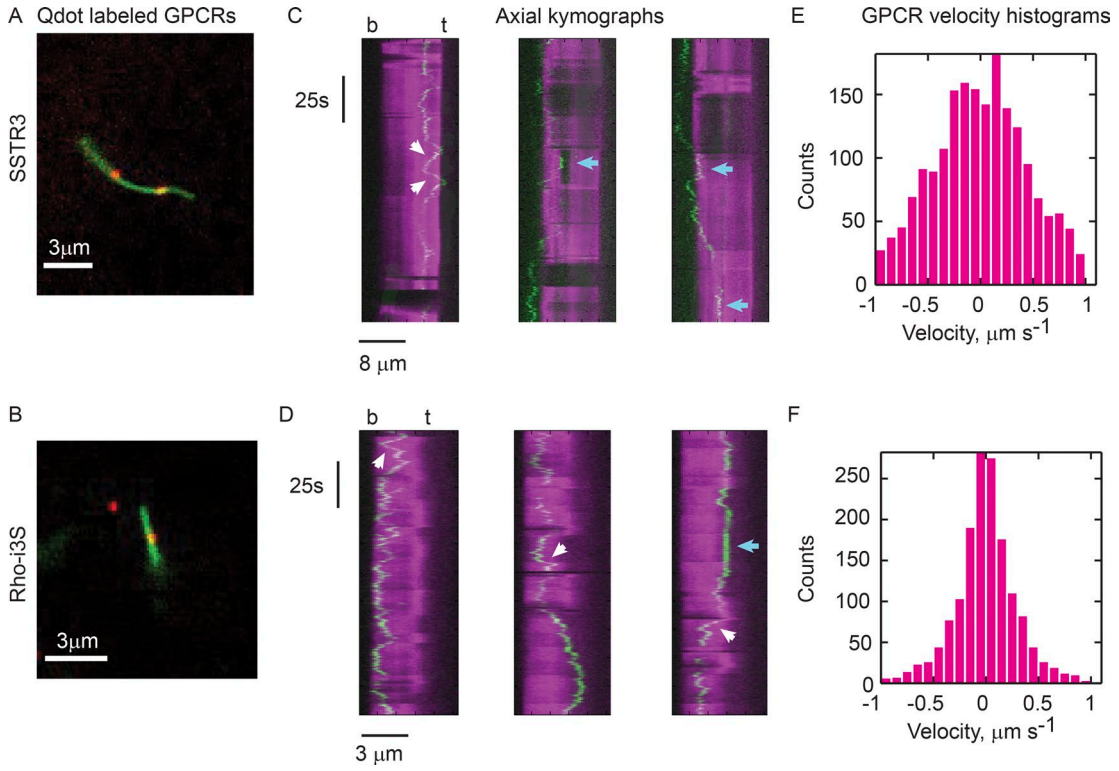

Figure S2. **Axial kymographs of GPCR tracking results reveal a mixture of Brownian motion, apparent processivity, and apparent binding to immobile structures. (A and B)** Stills from videos of a myc-SSTR3-EGFP containing cilium (A) and a myc-Rhoi3S-EGFP containing cilium (B), each showing the ensemble distribution of GPCRs (green) and the position of individual Qdot625 labeled GPCRs (red; Videos 3 and 4). **(C and D)** Kymographs of individual Qdot GPCRs shown in A and B. The distribution of the EGFP signal is overlaid in magenta as a reference. Blue arrows indicate regions of low mobility. White arrows indicate regions of apparent processive movement. Cilium base position (b) was determined by centrin2-BFP expression; t, position of cilium tip. **(E and F)** Instantaneous axial velocity histograms. Anterograde velocities are positive; retrograde are negative. Note the symmetry of the histograms, indicating that the distribution of velocities is essentially the same in the anterograde and retrograde directions. myc-Rhoi3S-EGFP, $n = 9$, eight individual cilia, four independent experiments; myc-SSTR3-EGFP, $n = 14$, eight independent experiments (see Table 1).

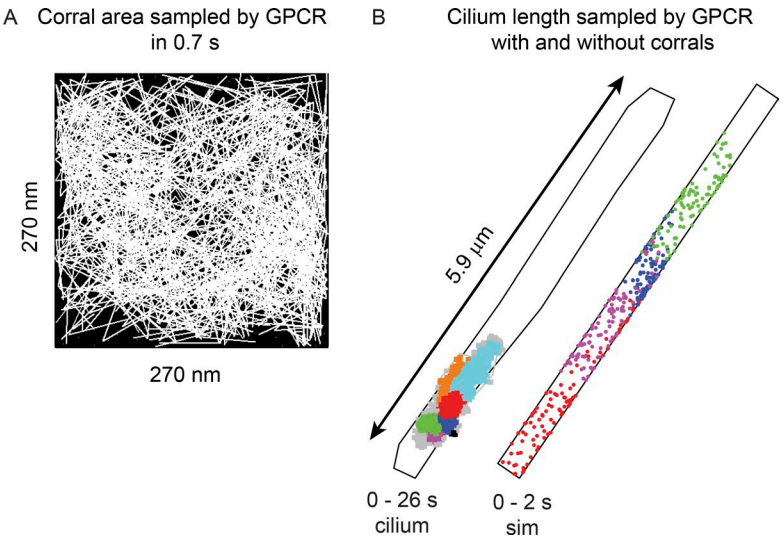

Figure S3. **Impact of corrals on sampling of the ciliary membranes by GPCRs. (A)** Corral area sampled by the GPCRs as determined by the line Wiener sausage analysis. A random walk simulation within a 270-nm^2 corral was executed with D_{cor} = 5.5 µm^2/s and t_{step} = 1 ms. Lines represent the path taken by the simulated GPCR between successive time steps. The width of the lines was 4 nm, the approximate diameter of the GPCRs within the membrane plane. The area covered by the lines was determined by the integral of the white pixels in the image and was divided by the total corral area to arrive at an area fraction sampled, A_s = 0.7 over the mean corral residence time T_r = 0.71 s. **(B)** Comparison of the cilium membrane space sampled by the Rhoi3S receptor from the high-speed tracking in Fig. 6, over the sampling interval of 26 s compared with the prediction from the unconfined model over a period of 2 s illustrates the dramatic impact of the corrals on GPCR sampling of the ciliary membrane space over long times and distances.

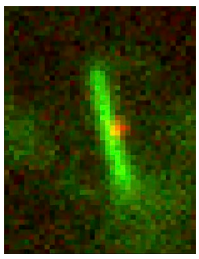

Video 1. **High-magnification video of the movement of Rhoi3S labeled with a Qdot625 shown in real time (3.33 fps).**

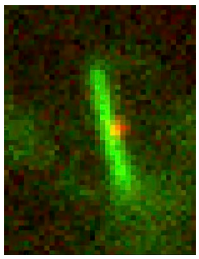

Video 2. **The same as Video 1 with tracking overlaid.**

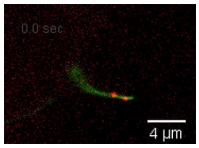

Video 3. **Low-magnification video of SSTR3 labeled with Qdot625 at 20 fps, accelerated 6.7-fold.**

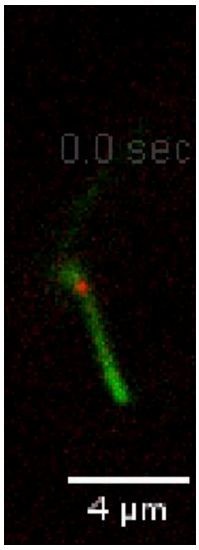

Video 4. **Low-magnification video of Rhoi3S labeled with Qdot625 at 20 fps, accelerated 6.7-fold.** Note the intensive sampling of the cilium tip during this time sequence.

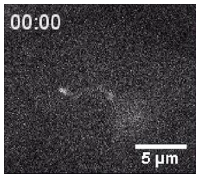

Video 5. **Tracking of IFT20-GFP at 20 fps, accelerated 6.7-fold.**

Video 6. **Output of a random walk simulation.** Left: Upper panel shows the positions of a theoretical GPCR after each time step on an unwrapped and flattened cilium membrane surface; lower panel shows the position of the theoretical GPCR (red dot) on the 3D cylindrical membrane. Right: Axial position of the theoretical GPCR as a function of time (axial kymograph), where the position has been blurred by a Gaussian kernel, with $\sigma = \sigma_{x,y}$ of the *psf*, to simulate the blurring of the Qdot by the optical system. Parameters of the simulation: l_{cyl} = 5 µm, D_m = 0.15 µm^2/s, t_s = 0.3 s. Video recorded at 24 fps, accelerated fivefold.

Video 7. **Output of a random walk simulation with stochastic motor coupling.** Parameters of the simulation: l_{cyl} = 5 µm, D_m = 0.15 µm^2/s, t_s = 0.3 s, P_m = 0.2, v_m = 0.6 µm/s, t_m = six time steps. Video recorded at 24 fps, accelerated fivefold.

Video 8. **Output of a random walk simulation with stochastic binding to immobile objects.** Parameters of the simulation: l_{cyl} = 5 µm, D_m = 0.15 µm^2/s, t_s = 0.3 s, P_b = 0.2, t_b = 10 time steps. Video recorded at 24 fps, accelerated fivefold.

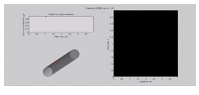

Video 9. **Output of a random walk simulation with semipermeable corrals.** Parameters of the simulation: l_{cyl} = 3.8 µm, D_m = 4.6 µm^2/s, t_s = 0.001 s, P_{bc} = 0.0024, l_{cor} = 0.25 µm. Note that marker color changes each time a corral boundary is crossed. Video recorded at 24 fps, accelerated fivefold.

Provided online as a ZIP file are the Matlab codes for the random walk and ensemble diffusion models.